Reduction of Dynamic Loads in Piston Compressors Through the Use of Mechanical Resonance

Wieslaw Fiebig and Willy Prastiyo

Wroclaw University of Science and Technology, Wroclaw, Poland
wieslaw.fiebig@pwr.edu.pl, willy.prastiyo@pwr.edu.pl

Abstract.

In reciprocating compressors that use the slider-crank mechanism, the input torque experiences significant fluctuations due to the inertial forces of the reciprocating components. In this paper, a technique to improve the dynamics of reciprocating compressors is presented using the phenomenon of mechanical resonance. The study involves a comparative analysis using multibody dynamics simulations (MBD), and comparisons of experimental investigations are performed in two main operating setups: 1. piston without an additional coil spring element; and 2. piston with an additional coil spring element. System performance is analyzed by examining the forces in the joints, the inertia torque, and the estimated power demand of the two main sets of components in various simulation scenarios considering different configurations of friction, pressure load, reciprocating mass, and spring stiffness. The MBD model is prepared and simulated in ADAMS. The findings of this study confirm that the resonance setup offers a significant advantage, exhibiting a lower inertia torque amplitude compared to the conventional setup, primarily attributed to the compensation of inertia forces by spring forces. Not only by the use of steel spring, in the case of the work of a compressor system, resonance can also be attained by the process of air compression. The stiffness of the air spring in the cylinder itself can be harnessed to achieve resonance. In this case, the influence of pressure on the natural frequency of the system is taken into account. To simulate the dynamics of fluid, an equivalent multidomain system of the model is made in Simcenter Amesim.

Keywords: resonance, vibration, slider-crank, mechanism, dynamics.

1. INTRODUCTION

Resonance is mostly known as an unwanted phenomenon in a mechanical system. Nevertheless, despite the common concern that the resonance phenomenon in most mechanical structures is undesirable, a number of studies show that resonance in a mechanical system can in fact be utilized to obtain a beneficial outcome. Franca & Weber [1] have studied the use of mechanical resonance in a drilling technique called resonance hammer drilling. In their study, the resonance phenomenon was used to increase the penetration rate (ROP) in hard rock drilling. Despotovic et al. [2] show that the vibratory

conveyor resonant mode with electromagnetic excitation consumed less energy when maintaining the system in the resonance state. Aiple, M., et al. [3] show that if the excitation frequency and the resonance frequency are the same, with a flexible (Series Elastic Actuator-based) hammer, teleoperators can reach peak velocities of more than 200% higher than peak velocities with a rigid hammer. Compared to a rigid hammer driven by the same velocity source, the peak velocity and peak energy of a flexible hammer are substantially higher when the mechanical resonance of the hammer is excited. Fiebig & Wróbel [4], based on their simulation and experiment, found that the impact machine that uses mechanical resonance with a resonant block and spring element has a significant reduction in energy demand compared to the conventional machine that uses slider-crank and flywheel coupling.

When a slider-crank mechanism is activated, in which the rotation of its crank drives the linear movement of the slider, the reaction torque arises when the slider translationally accelerates or decelerates [5]. A higher fluctuation of the reaction torque and forces on joints due to inertial forces [6] can, in fact, result in higher energy dissipation [7] that arises from joint friction and internal stresses of the components. In the end, higher energy dissipation will lead to lower system energy efficiency [8].

In this paper, the approach to improving the dynamics of the slider-crank mechanism will be done through the modification of the conventional slider-crank design [9, 10] and the arrangement of the system operation within the resonance frequency. In particular [11], the reciprocating compressor (or piston compressor) is discussed as a practical study example because it represents the common application of a slider-crank mechanism that has varying external loads [12, 13]. The numerical simulation method, which includes multibody dynamics (MBD), is used to model, analyze, and estimate the performance of the designed system. In addition, a physical prototype is built for verification. The contributions of this study are as follows: (a) The method of utilizing mechanical resonance in the slider-crank mechanism is described, especially for the case of a reciprocating compressor. (b) Comparative results of the system with and without the use of mechanical resonance are presented.

2. MODELING OF THE RECIPROCATING COMPRESSOR

As shown in Figure 1, the presented model consists of the crankshaft, as the crank; and the crosshead, push rod, and piston. The coil springs envelope the rails, fixed to the main frame and the crosshead so that, at equilibrium position, the slider is in the middle of the stroke. Moreover, since MSC ADAMS cannot simulate the dynamics of the fluid, the Simcenter Amesim model has been developed to obtain the compression forces on the piston.

The model in Simcenter Amesim will be shown in Fig. 2. The electric motor rotates the crankshaft, which is then converted by the connecting rod into translational motion to move the crosshead and the piston. When the piston moves from the TDC (top dead centre) to the BDC (bottom dead centre), the pressure differential causes the inlet valve to open; the air is sucked into the cylinder. The air inside the cylinder is then pumped out through the outlet valve into the tank. A relief valve is used to limit the upstream pressure within the pneumatic circuit, thus protecting the pneumatic components from overpressure. Each simulation step size and duration in the multidomain system should be synchronized with the multibody dynamics simulation.

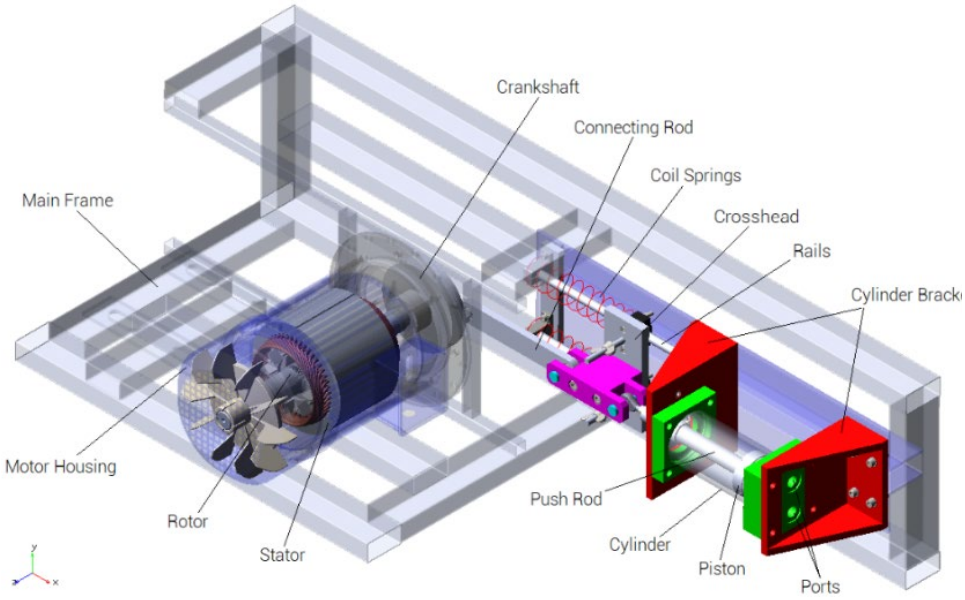

Figure 1: CAD-MBD model of the reciprocating compressor prototype. The electric motor is adapted from [7].

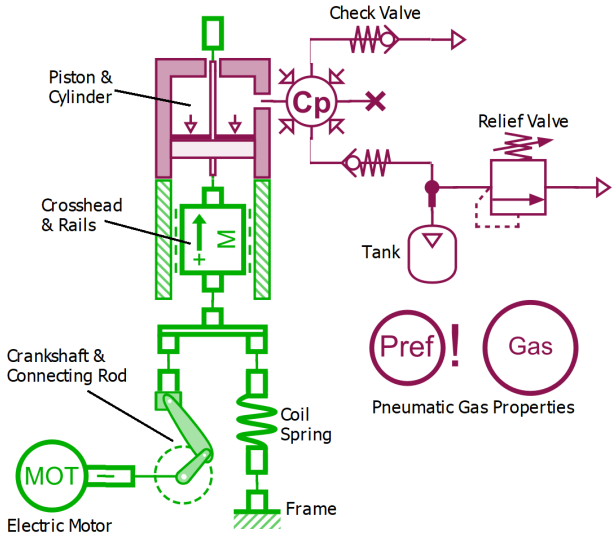

Figure 2: Sketch of the reciprocating compressor prototype.

The initial position of the crank (in Figure 2) is set at 0 °, which means that the piston is initially located at TDC. The cycle starts from the suction stroke, TDC to BDC (0° to 180 ° of the crank); followed by the compression stroke, BDC to TDC (180° to 360° of the crank). Compressed air is stored inside the tank and pressure builds gradually until the relief valve

cracks pressure. When the crack pressure of the relief valve is set at 8.7 bar, for example, the maximum pressure achieved inside the cylinder is about 8.84 bar and the force pushing down the piston reaches around 2500 N (Figure 3).

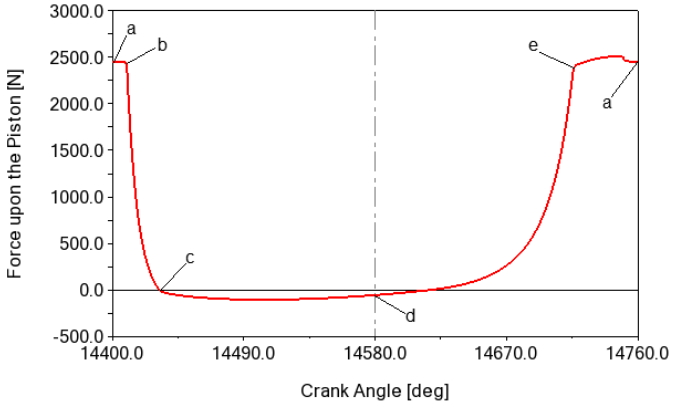

Figure 3: Force acting on the piston in one cycle (0° to 360 ° of crank), expansion (a-c), effective suction (c-d), compression (d-e), and discharge (e-a).

Table 1: Parameters of the simulations.

Components	Parameters	Value
Crankshaft & connecting rod	Initial angular position of the crank	0 degree
	Radius of the crank	50 mm
	Length of the connecting rod	168 mm
Piston & cylinder	Piston diameter	60 mm
	Chamber dead volume	0.62 L
Source of atmospheric pressure and temperature	Temperature	293.15 K
	Reference pressure	1.013 barA
Tank	Volume	1 L
Generic Gas Definition	Specific heat ratio	1.4
	Specific gas constant	287 J/kg/K
	Absolute viscosity	0.0182 cP
	Thermal Conductivity	0.0264 W/m/K
	Enthalpy of Formation	−125.53 J/mol
	Definition of properties	air, perfect gas

Part	Mass [kg]	Moment of Inertia [kg.mm^2]			Connected with	Joint
		I_{xx}	I_{yy}	I_{zz}		
Main frame	24.59	3.08×10^6	2.80×10^6	5.76×10^5	Ground	Fixed
Stator	2.80	1.103×10^4	8562.18	8555.26	Motor housing	Fixed
Connecting rod	0.15	451.95	441.64	12.76	Crankshaft	Revolute
					Crosshead	Revolute

Crankshaft	0.85	1350.89	798.75	772.66	Connecting rod	Revolute
					Rotor	Fixed
Cylinder	1.53	4056.40	4054.44	1688.46	Cylinder brackets	Fixed
					Piston	Cylindrical
Front cylinder bracket	4.13	1.59×10^4	1.07×10^4	7412.01	Main frame	Fixed
					Cylinder	Fixed
Motor housing	2.12	1.69×10^4	1.62×10^4	1.37×10^4	Main frame	Fixed
					Rotor	Fixed
Piston (including pin)	0.25[b]	335.87	292.34	290.84	Push rod	Fixed
					Cylinder	Cylindrical
Push rod	0.25[b]	2358.69	2357.44	35.95	Piston	Fixed
					Crosshead	Revolute
Rail	1.22	1.89×10^4	1.66×10^4	2664.15	Main frame	Revolute
					Crosshead	Translational
Rear cylinder bracket	3.93	1.90×10^4	1.09×10^4	1.01×10^4	Main frame	Fixed
					Cylinder	Fixed
Rotor	2.59	1.32×10^4	1.32×10^4	2554.61	Crankshaft	Fixed
					Motor housing	Revolute
Crosshead	*varied*	4850.21	4338.28	3509.18	Rail	Translational
					Connecting rod	Revolute
					Push rod	Revolute

3. SIMULATION RESULTS

3.1. Dynamic Torque without Load Pressure

Figure 4 shows that the setup without springs and without pressure has a progressive increase in dynamic torque as the angular velocity increases. On the other hand, the setup in which the springs are installed has a lower magnitude of dynamic torque at its resonant frequency of around 84.69 rad/s. At resonance frequency, the system effectively stores and transfers energy between the kinetic energy of the slider and the potential energy of the spring so that the torque and the required effort for the crankshaft to rotate are significantly lower than in any other angular velocity.

Figure 5 presents the graphs of power consumption vs. angular velocity, shown only in positive values that represent the magnitude of the power demand for the system to operate. The setup with spring shows that at a resonant frequency, the magnitude of power demand is about 0.3 kW, unlike the conventional one, which might require power at around 1.4 kW.

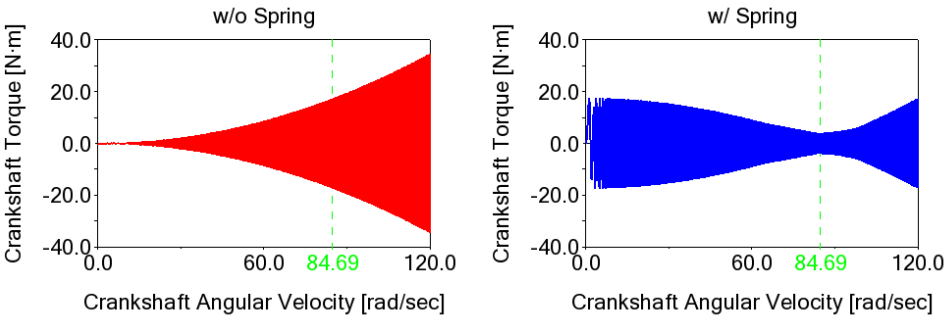

Figure 4: Torque vs. angular velocity curves without spring and with spring (data from Table 1, m=1.5 kg), without pressure load.

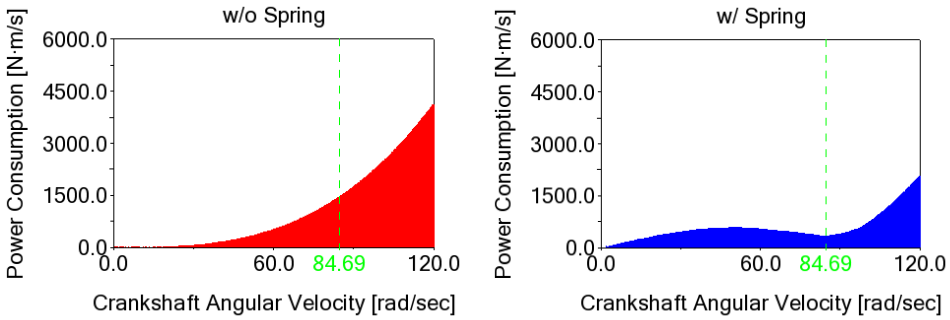

Figure 5: Instantaneous power demand vs. angular velocity curves, data from Table 1, m=1.5 kg), without pressure load

3.2. Dynamic Torque with Load Pressure

Several simulations are done to generate the force data in the example case of 0, 2.5, 5, 7.5 and 10 bar of air pressure. Figure 3 shows the force on the piston during the air suction and compression process within one cycle. Based on these simulations, the force data on the piston versus the angular position of the crank are imported into the MBD simulations, used as the input value of the applied force, which is placed at the top of the piston as a function of the angle of the crank.

Figure 6 shows the simulation results based on the data set defined in Table 1. It can be observed that when the crankshaft is operated at the resonant frequencies (denoted by the green line), the peak and RMS torque of the setup with spring is noticeably lower. Nevertheless, not only the setup with spring, it can be observed that the setup without spring also has a narrow torque region around its own resonant frequency since the compression of the air itself acts as the air spring compression. In this practical example, air compression can also be utilized to provide resonance, usually at lower frequencies. In case of working with a system that has an adjustable prime-mover angular velocity, if the resonance has been achieved at its own compression load, a spring might not be needed, and resonance can still be attained; otherwise, the installation of a spring with adjusted stiffness might be used to

match the resonance frequency with the available prime-mover angular velocity. In addition, the influences of both the mass of the reciprocating bodies and the resonance operating speed (that is adapted by the proper spring stiffness) are discussed in the paper [14].

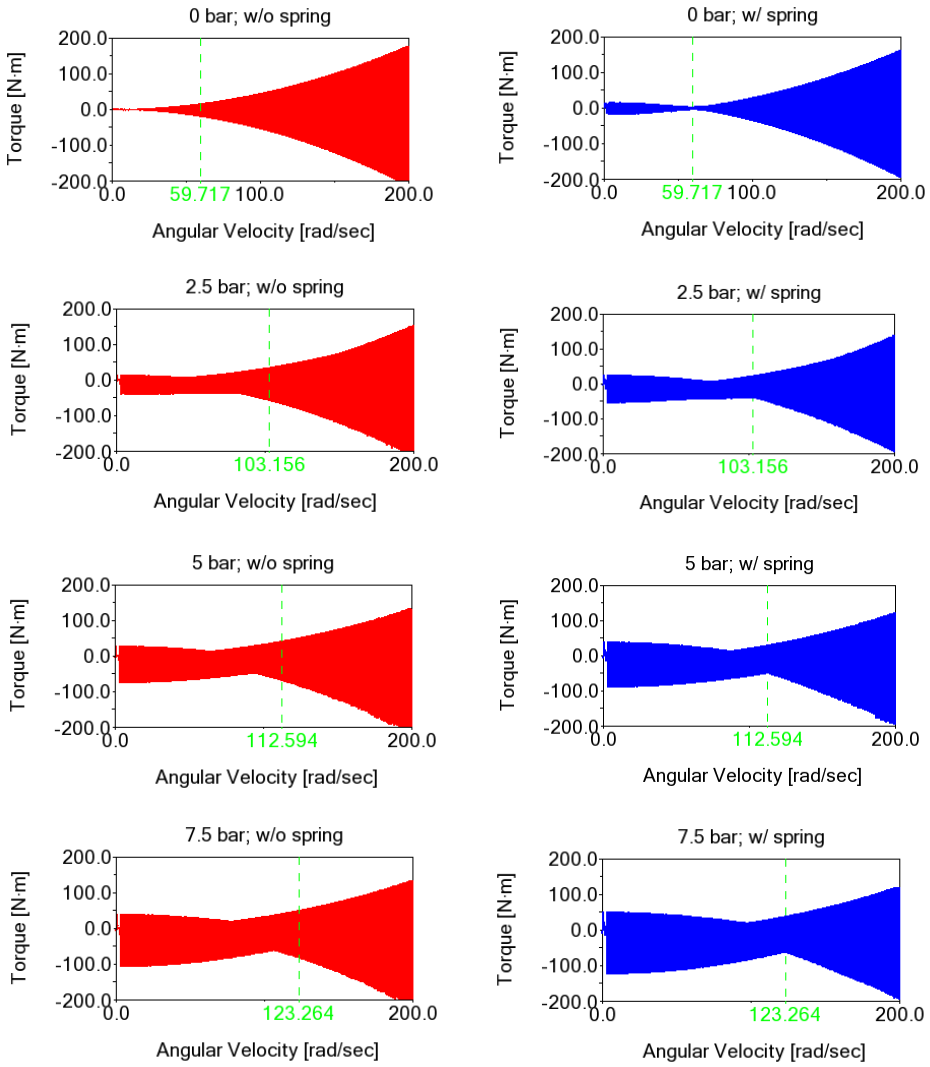

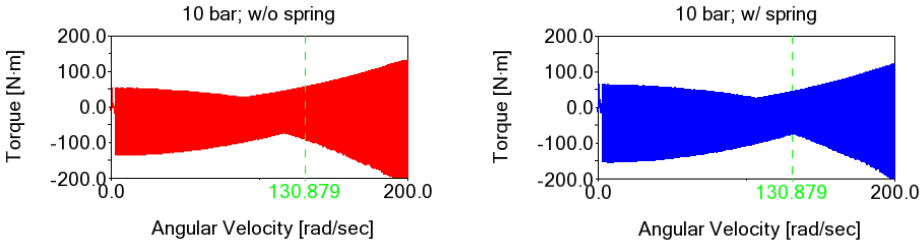

Figure 6: Torque vs. angular velocity graphs. Red- setup without spring, blue- setup with spring, data from the Table 1, M=3 kg, k= 6,25 N/m

If the resonance angular frequencies resulting from air springs in the compressor operating pressure range are too low, a steel spring should be used, ensuring a higher resonance frequency. In electric drives with variable speed, a control system can be used that adjusts the motor speed to the resonance. Selection of the appropriate stiffness in relation to achieving the resonance conditions is possible on the basis of the dynamic system simulation method presented in this paper. Equivalent spring stiffness is defined as:

$$k_e = k_s + k_g \tag{1}$$

where
k_s—mechanical spring stiffness;
k_g—gas spring stiffness.
The stiffness of the gas spring is nonlinear [7] and depends on the pressure and stroke of the piston $k_g = f(p, s)$.

$$k_g = E\frac{A^2}{V} \tag{2}$$

where:
E_p - bulk modulus depending on pressure.
A - piston surface
V - fluid volume depending on the position of the piston.

Depending on the required RPM of the electric motor (constant/variable), the equivalent spring stiffness can be obtained in the following way:

- For low-speed compressors, only a gas spring can be used, depending on the discharge pressure range.
- For high-speed compressors, an additional set of steel springs can be used to achieve resonance conditions.

The use of constant-speed motors requires a relatively exact selection of the equivalent stiffness in the compressor. By variable speed drives (VSD), resonance conditions can be achieved using, i.e. the appropriate frequency tracking control system [15].

4. EXPERIMENTAL INVESTIGATIONS

As shown in Figure 7, the physical prototype was built similar to the MBD model except for the drivetrain and the spring attachment. The prototype consists mainly of the compressor section and the electric drive section. The relief valve can adjust the level of external loads, that is, the magnitude of air pressure, on the slider.

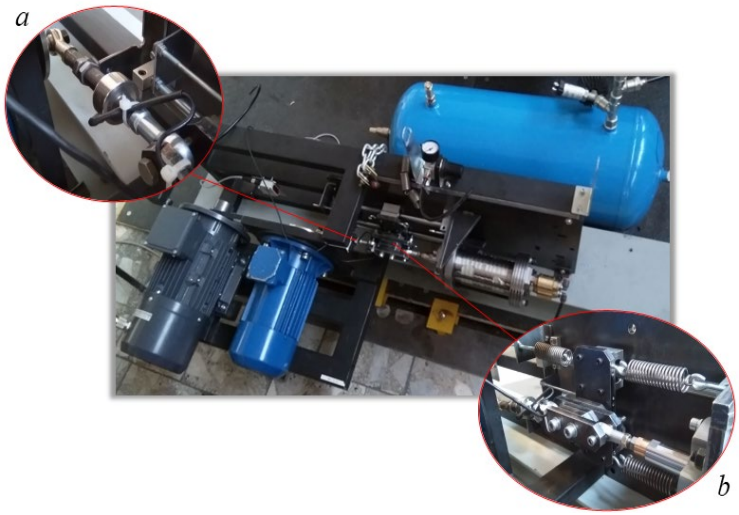

Figure 7: Physical prototype. Zoom in (a) force sensor on the joint of the connecting rod and (b) crosshead and springs.

The electric drive system consists of a three-phase motor, PLC, VFD, relay, circuit breaker, switches, cables, and control panel box. The assembled control unit in this system is programmed for the possibility of the motor to operate at a constant specified speed and steadily increasing speed (ramp function) to provide the sweep function to the slider. In the following, the resonance speed of the system can be identified. The force sensor was mounted on the connecting rod. Finally, sets with and without springs are tested to compare their forces on the joints of the connecting rod.

The test results are shown in Figure 8 and their essential data are presented in Table 2. It can be observed that all spring sets have a narrow force region around the resonance speed. Almost the same as in simulation, at the pressure 0 bar, the setup with spring provides about 60.34% reduction in the peak-to-peak force at resonance when no pressure load is involved (and no valves are installed). The attachment of the valves poses as an external load, so that the peak-to-peak force is reduced by 20.9%. This result underscores the important role of pressure losses that occur in the inlet and outlet valves in obtaining the highest positive resonance effect.

As demonstrated in the simulations, compression of the air itself takes effect as a spring compression. Even without any coil spring installed, a narrow force region can be observed in the setup without a spring. At 1 bar, the reduction of force goes down to 6.26% and 16.24% at 126.4 rad/s (1207 rpm) and 141.8 rad/s (1354 rpm) which are the resonance frequencies of both the setup without spring and the setup with spring, respectively. At the pressure 1 bar, if both sets are run and compared at their own resonant speed, that is, 126.4 rad/s for the conventional setup and 141.8 rad/s for the resonance setup, the difference in peak-to-peak force is less significant; about 1.53%. Therefore, in the air compression process, the spring may or may not be installed after the available system parameter. As long as the system is run at resonant frequency, enhancement of the system dynamics might be achieved.

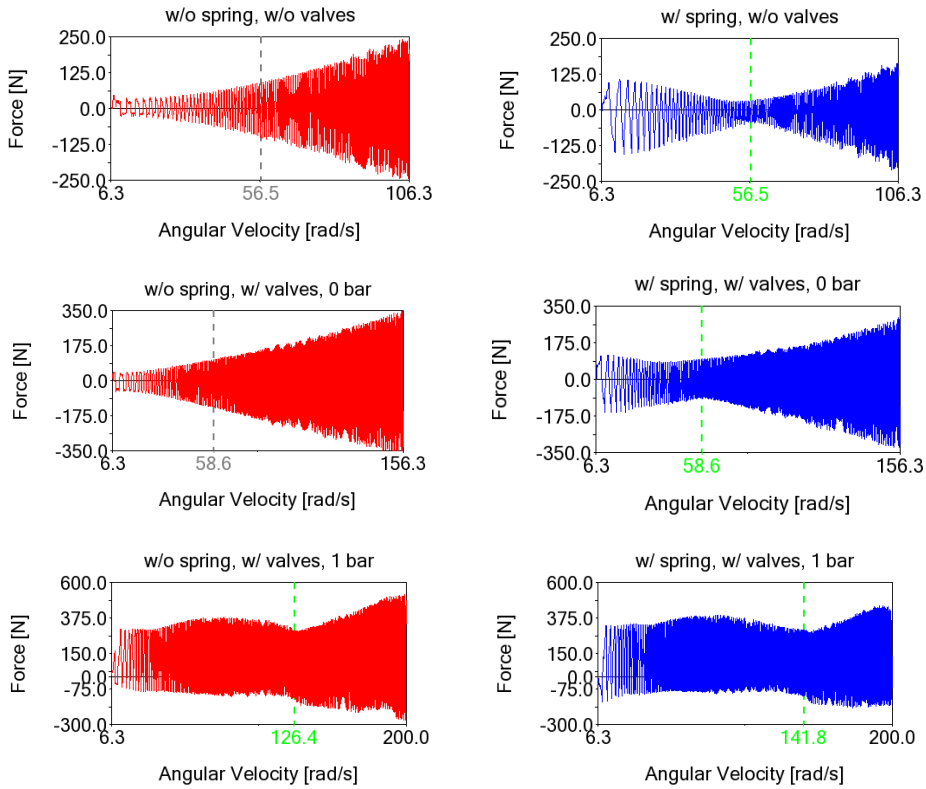

Figure 8: Force–angular velocity graphs of the set-up without spring (red) and with spring (blue). The force is measured on the connecting rod as shown in Figure 6(a). Reciprocating mass = 3.9 kg, spring stiffness = 2.5 kN/m.

Table 2. Comparison of the force on the connecting rod of the physical prototype.

Load [bar]	**Resonant frequency [rad/s]**	**Pulling force [N]**		**Pushing force [N]**		**Peak-to-peak force amplitude [N]**		**Decrease in the peak-to-peak amplitude of the force [%]**
		w/o spring	w/ spring	w/o spring	w/ spring	w/o spring	w/ spring	
w / no valves	56.5	−99.8	−43.9	93.2	32.6	193.0	76.6	60.3
0	58.6	−134.6	−92.0	106.1	98.3	240.7	190.4	20.9
1	126.4	−133.2	−84.0	295.0	317.4	428.3	401.5	6.3
1	141.8	−181.6	−121.0	321.8	300.7	503.5	421.8	16.2

5. CROSS-HEAD COMPRESSORS

The described method for reducing the force and torque pulsation can be used in industrial crosshead compressors. These types of compressors are often used i.e. for the compression and transportation of natural gas. In such compressors, the mass forces reach high values. The reciprocating movement is performed by pistons together with a crosshead, which are used to reduce the piston slap and increase the tightness. Due to the wear of individual elements related to friction in the joints, each reduction in the amplitude of variable loads contributes to reducing friction forces, wear, and thermal losses.

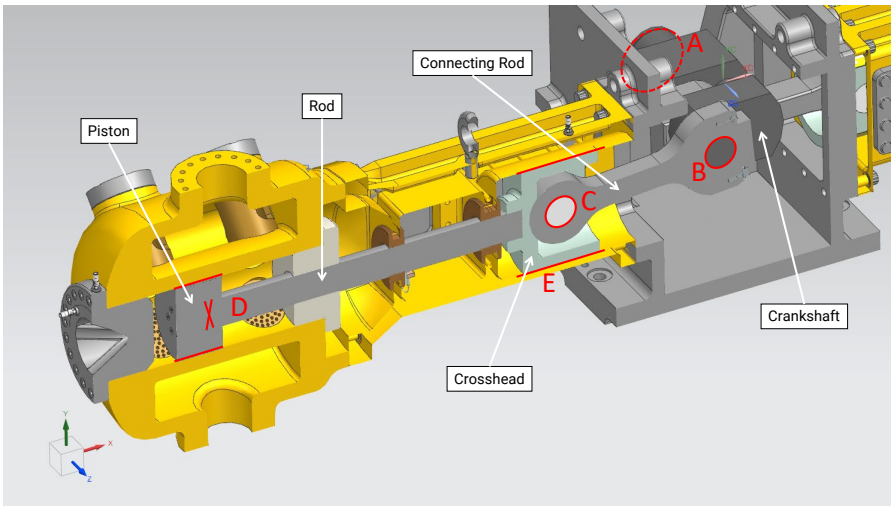

Figure 9. Cross section of the cross head compressor with the joints marked in red, Ariel compressor [16]. Reciprocating masses of 272.4 kg, crank length of 82.56 mm, connecting rod length of 533.4 mm, piston diameter of 254 mm, piston rod diameter of 101.4 mm

5.1. Dynamic Torque with Load Pressure

Industrial crosshead compressors are usually double-acting. The double-acting compressor compresses the air on both the up-stroke and the down-stroke of the piston, doubling the capacity of a given cylinder size.

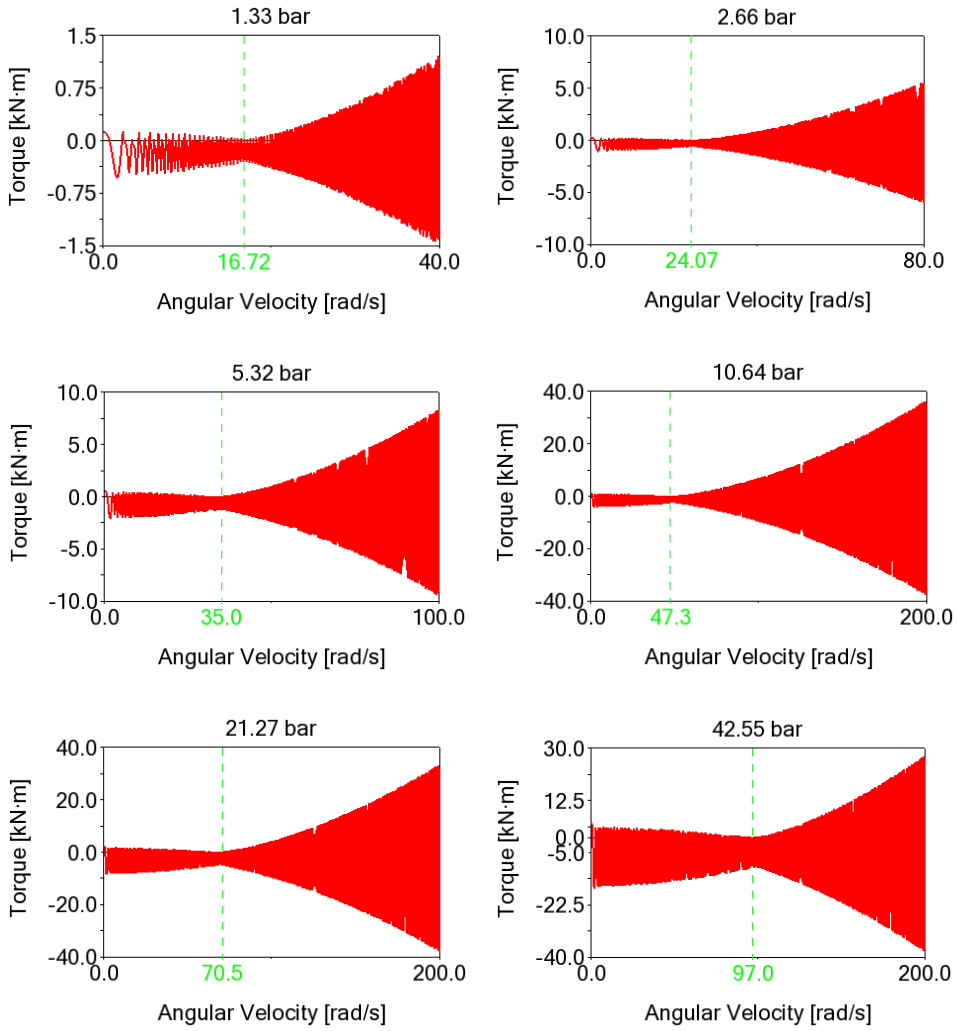

Figure 10: Torque vs. angular velocity graphs for a cross-head compressor without spring. Data from Figure 9.

The amplitudes of the torque and forces in the joints in the resonac are much smaller than for velocities above and below resonance. For higher resonance frequencies, this effect is even more visible in Figures 10 and 11.

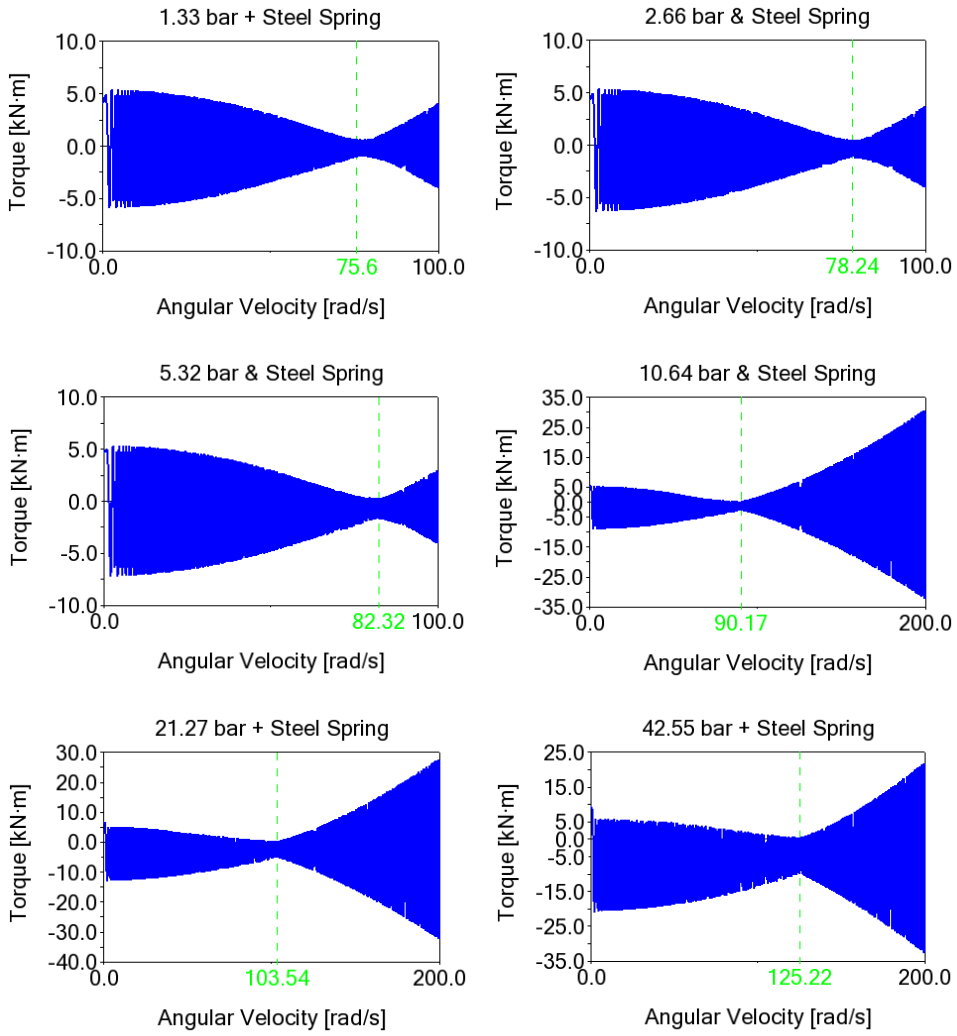

Figure 11: Torque vs. angular velocity graphs for the crosshead compressor with spring. Data from Figure 9, spring stiffness 1500 kN/m.

5.2. Dynamic Forces on Joints

Figure 12 shows the forces in the cross-head compressor joints before resonance (blue line), during resonance (green line) and after resonance (red line). It can be observed that in the resonance state the force amplitudes are much smaller (except for the connection between the piston and the piston rod).

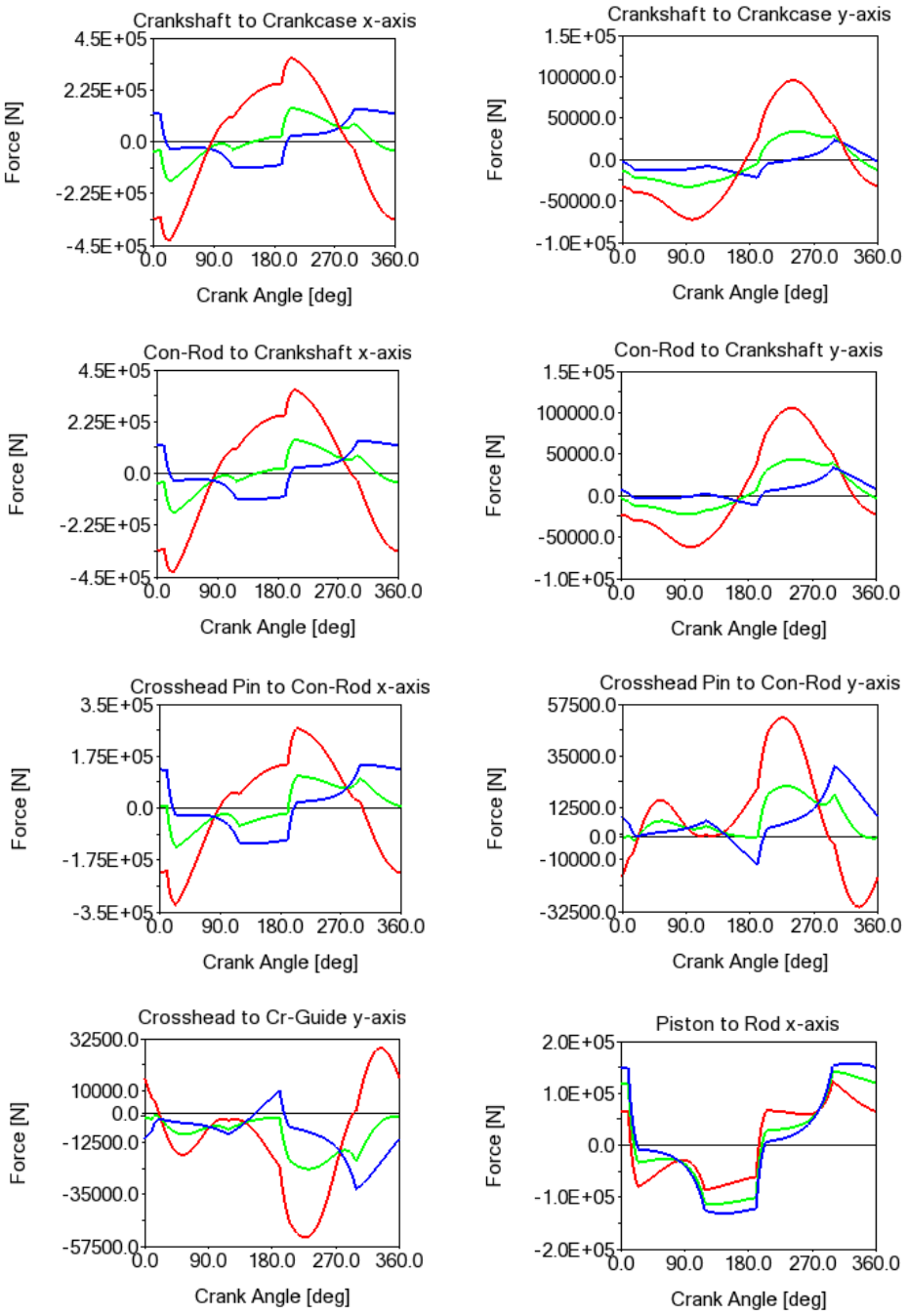

Figure 12: Forces on revolute and translational joints (arbitrary vs. resonance); no load and friction, stage 2 of compression. operating speed: red=135.5 rad/s, green=85.5 rad/s (narrowest region), blue=35.5 rad/s.

Figure 13 shows the dependence of the resonant angular velocity on the cylinder pressure for the versions without a spring and with a steel spring. In the absence of a steel spring, there is a nonlinear increase in angular velocity as a result of pressure. By using steel springs, higher resonance frequencies can be obtained. Therefore, their use would be appropriate for high-speed cross head compressors.

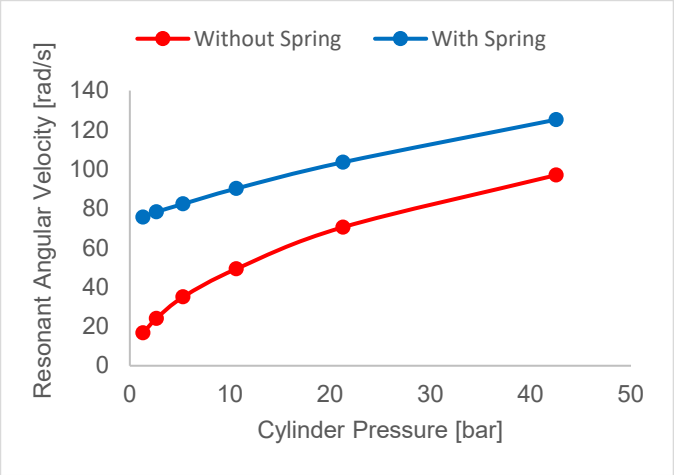

Figure 13: Resonant angular velocity vs. cylinder pressure of the crosshead compressor data from Figure 9, steel spring stiffness of 1500 kN/m

6. CONCLUSIONS

In this paper, a technique for improving the dynamics of the slider-crank mechanism is presented using the phenomenon of mechanical resonance. A comparative study towards the resonance and conventional operation is done using MBD simulations. A reciprocating compressor model is explored as a practical case study example, representing the application of a slider-crank mechanism.

It is found that the introduction of a spring element that can store and transfer back the potential energy in the slider-crank mechanism can provide a positive effect of resonance. The input torque on the crank shaft and the forces on all rotating joints of the setup run at resonance provide lower peak and RMS values (narrow region) compared to the conventional operation. The setup without a coil spring also presents a narrow torque region around the resonant frequency, since the process of air compression itself acts as the air spring compression. Whether or not the system uses the coil spring, as long as it is run at the resonant frequency, the advantageous result of resonance can be achieved.

If a particular pressure demand is required to maintain resonance, the angular velocity of the driving unit should be changed accordingly. In a future study, a control algorithm could be developed to improve the capability of the resonance slider-crank system presented, for example, using a frequency tracking control system [9]. Although the practical example presented in this article is only limited to the process of air compression, studying the use of resonance in the slider-crank mechanism for other applications would be very much worthwhile.

The simulation results indicate that an increase in equivalent spring stiffness (air spring plus steel spring) leads to higher power efficiency. Also the rotating joints at resonance exhibit lower peak and RMS values of forces. Finally, experimental verification of the slider-crank mechanism at resonance demonstrates a behavior equivalent to that in simulations. Based on the analysis, it can be concluded that controlled mechanical resonance can effectively reduce inertia load magnitudes in reciprocating compressors.

The innovative method proposed in the article has great application potential, especially in industrial cross-head compressors, in which the share of inertia forces is greater, and the forces occurring in the crank slider mechanism determine the wear and durability of these compressors.

7. REFERENCES

[1] Franca, L. F., & Weber, H. I. Experimental and numerical study of a new resonance hammer drilling model with drift. *Chaos, Solitons & Fractals,* **21**(4), 789-801, (2004).

[2] Despotovic, Z., Sinik, V., & Ribic, A. The impact of switch-mode-regulated vibratory resonance conveyors with electromagnetic drive on the power supply network. *2012 15th International Power Electronics and Motion Control Conference (EPE/PEMC)*, (2012).

[3] Aiple, M., Smisek, J., & Schiele, A. Increasing Impact by Mechanical Resonance for Teleoperated Hammering. *IEEE Transactions on Haptics*, **12**(2), 154–165, (2019).

[4] Fiebig, W. & Wróbel, J. Energy accumulation in mechanical resonance and its use in drive systems of impact machines. *Archives of Civil and Mechanical Engineering,* **20**(1), (2020).

[5] Ni, L., Huang, Y. Y., & Zhou, C. K. The dynamic simulation of Engine Slider-Crank mechanism based On ANSYS and Adams. *Advanced Materials Research, 842*, 347-350, (2013).

[6] Hroncová, D., Binda, M., Šarga, P., & Kičák, F. Kinematical analysis of crank slider mechanism using MSC ADAMS/View. *Procedia Engineering, 48*, 213-222, (2012).

[7] Bödrich, T. (2006). System and Component Design of Directly Driven Reciprocating Compressors with Modelica. Modelica 2006, September 4th – 5th

[8] Daniel, G.B.; Cavalca, K.L. Analysis of the dynamics of a slider–crank mechanism with hydrodynamic lubrication in the connecting rod–slider joint clearance. *Mech. Mach. Theory* **2011**, *46*, 1434–1452.

[9] Ni, L.; Huang, Y.Y.; Zhou, C.K. The dynamic simulation of Engine Slider-Crank mechanism based on ANSYS and ADAMS. *Adv. Mater. Res.* **2013**, *842*, 347–350.

[10] Arakelian, V. Design of Torque-Compensated Mechanical Systems With Two Connected Identical Slider-Crank Mechanisms. *J. Mech. Robot.* **2021**, *14*,

[11] Hroncová, D.; Binda, M.; Šarga, P.; Kičák, F. Kinematical analysis of crank slider mechanism using MSC ADAMS/View. *Procedia Eng.* **2012**, *48*, 213–222.

[12] Arakelian, V.; Briot, S. Simultaneous inertia force/moment balancing and torque compensation of slider- crank mechanisms. *Mech. Res. Commun.* **2010**, *37*, 265–269.

[13] Pishvaye Naeeni, I.; Keshavarzi, A.; Fattahi, I. Parametric Study on the Geometric and Kinetic Aspects of the Slider-Crank Mechanism. *Iran. J. Sci. Technol. Trans. Mech. Eng.* **2018**, *43*, 405–417.

[14] Fiebig W, & Prastiyo W. Utilization of Mechanical Resonance for the Enhancement of Slider-Crank Mechanism Dynamics in Gas Compression Processes. *Energies*, **15**(20):7769, (2022). https://doi.org/10.3390/en15207769.

[15] Xu, W., Wang, Q., Li, X., Liu, Y., & Zhu, J. A novel resonant frequency tracking control for linear compressor based on MRAS method. *CES Transactions on Electrical Machines and Systems*, **4**(3), 227–236, (2020).

[16] Troy. (2012). CAD File of Ariel 6 Throw Compressor. [Online] available: https://grabcad.com/library/ariel-6-throw-compressor.